Journal of Applied Geophysics 204 (2022) 104743

Contents lists available at ScienceDirect

Journal of Applied Geophysics

journal homepage: www.elsevier.com/locate/jappgeo

The LAMA system: A “smart” magnetometer network for harbour protection

Maurizio Soldani [a,*], Osvaldo Faggioni [a,b], Rodolfo Zunino [b], Alessandro Carbone [c], Marco Gemma [c]

[a] *Istituto Nazionale di Geofisica e Vulcanologia, Via di Vigna Murata 605, 00143 Roma, Italy*
[b] *University of Genoa, Department of Electric, Electronic, Telecommunication Engineering and Naval Architecture, Via all'opera Pia 11A, 16145 Genova, Italy*
[c] *SkyTech Srl, Via delle Pianazze 74, 19136 La Spezia, Italy*

ARTICLE INFO

Keywords:
Marine geophysics
Environmental magnetism
Magnetic anomaly detection
Underwater magnetic systems
Harbour protection
Time series analysis

ABSTRACT

This work describes the development of an underwater anti-intrusion system based on a magnetometer self-informed network, whose purpose is to detect the presence of threats in the proximity of critical infrastructures (e.g, terrorist divers in harbours). In this context, the magnetic network fills the gaps of sonar systems at the critical boundaries of the water volume to be controlled (sea bed, docks, …), where acoustic performances deteriorate due to reflections and attenuations. The system operates in a port-protection scenario, characterized by a medium-high environmental magnetic noise that can hide the diver signal (a diver is a weak, quasi-point-like, moving source). The magnetometer network processes two inputs: the environmental magnetic noise and a signal including the target magnetic signal superimposed to the same noise; the frequencies of a diver signal lie within the noise band, hence frequency filtering proves inadequate for noise removal. The basic idea underlying the system is to measure and use the noise itself to filter the overall signal; measuring noise supports a background-subtraction process that allows to extract the target signal and therefore detect the threat presence. The effectiveness of the procedure depends on the positions of magnetometers: sensors must be close enough to one another to measure the common background noise, and, at the same time, should be distant enough from one another so that just one sensor can measure the target signal. To generate alarms when a threat is detected, a real-time software application processes data and activates a visual and acoustic alarm upon identification of a magnetic anomaly. Sea trials carried out in port areas provided extremely satisfactory results in the detection of intruders. The paper presents experimental results obtained during the method validation tests, when intruders were moving in the surrounding undersea environment.

1. Introduction

Terrorist events that characterized the beginning of this millennium stimulated a new research topic, whose goal is to develop systems for defending critical infrastructures, since the latter are considered as most exposed to risks of attacks (industrial plants, military bases, ports and airports, etc.). This area of study involves research centres, universities, institutions, armies, navies and industries from all over the world.

In maritime areas, the line of research named harbour (or port) protection aims to detect the presence of threats, such as terrorist divers, in ports and coastal areas. The systems traditionally used for this purpose in the underwater environment rely on sonar devices. These approaches, however, tend to lose their effectiveness when operating near the seabed or docks, due to (possibly multiple) reflections of the acoustic impulses. To compensate for this, underwater magnetic surveillance systems have been developed, which are complementary to the acoustic ones because they better work where the performance of sonar systems decay (and vice versa) (Dobkowski et al., 2007; Dobkowski et al., 2008; Lipovský et al., 2015; Liu et al., 2015; Tian, 2011; Wahlström and Gustafsson, 2014; Zhao et al., 2021).

A team of Italian researchers from INGV (National Institute of Geophysics and Volcanology) and University of Genoa developed, over the past fifteen years, an anti-intrusion underwater system prototype based on the measurement of the magnetic field in the sea, mostly in the

---

* Corresponding author.
E-mail addresses: maurizio.soldani@ingv.it (M. Soldani), osvaldo.faggioni@ingv.it, osvaldo.faggioni@unige.it (O. Faggioni), rodolfo.zunino@unige.it (R. Zunino), carbone.a@skytechnologies.it (A. Carbone), gemma.m@skytechnologies.it (M. Gemma).

https://doi.org/10.1016/j.jappgeo.2022.104743
Received 19 October 2020; Received in revised form 4 February 2022; Accepted 16 June 2022

context of projects funded by Ministry of Defence – National Plan for Military Research. A linear array of interconnected, passive magnetometers measure the surrounding magnetic field, without emitting any signal (Faggioni et al., 2008; Faggioni et al., 2009c; Gabellone et al., 2007; Gavazzi et al., 2019; Hirvi et al., 2007; Serkerov et al., 1996).

In a preliminary version (the CAIMAN[1] Project, with industrial partner WASS, now Leonardo SpA), the system included commercially available magnetometers and cables, and could operate on both land and underwater. That architecture exhibited some critical issues, namely, the high cost of legacy sensors, and the fact that a specific cable connected to each sensor. Thus the system included N cables for N sensors, and this complicated the deployment procedures.

The second release (LAMA[2] and LAMA2.0 Projects, with industrial partner SkyTech, La Spezia), adopted self-produced proprietary sensors (thus lowering costs) and one cable traversing all sensors of the system (smaller size). The reduced implementation costs allowed to include a larger number of sensors, and therefore to protect wider port entrances. The cost per sensor decreased from approximately 2500 € down to 500 €. As a result, the overall deployment envisioned systems five times longer. The lower number of cables, on the other hand, reduced the bulk of the system and made the deployment operations at sea much easier and faster.

The magnetic chain is usually deployed on the seabed (but it can also be buried or placed near the base of a pier) and can detect, for example, the presence of a diver swimming near the sensors. The Magnetic Anomaly Detection method discriminates the signal generated by the intruder's equipment ("anomaly" or "singularity") from the surrounding environmental magnetic noise ("background") (Faggioni et al., 2018; Faggioni et al., 2009a; Nasta et al., 2015; Szarka, 1988).

The paper describes the architecture of the system and shows the results obtained during the sea trials performed in February 2019 in La Spezia harbour, Italy (the goal of the test was to validate the system by detecting the presence of underwater threats).

2. Material and methods

2.1. Methodology

The system operates in a port-protection scenario, characterized by medium-high environmental noise with a relevant man-made magnetic noise component (e.g., industry or vessel-originated noise) that can cover the diver signal. The acquisition network includes a magnetic underwater array, above which professional divers performed multiple approach runs (NOAA et al., 2010).

Divers are weak, quasi-point-like, moving magnetic sources, mostly due to scuba tanks and equipment, which change the local, environmental magnetic field lines: a differential processing approach can detect weak signals buried in a high environmental magnetic noise. Conventional filtering techniques, such as those based on the Fourier Transform, prove inadequate because the typical frequencies of diver signals (depending of swimming speed) lie within the noise band; likewise, signal amplitudes (varying with the diver's distance from sensors) compare with the noise amplitude (De Vuyst and De Meyer, 1973).

The system discriminates between two different inputs: the environmental magnetic (background) field (natural plus artificial noise), and the superimposition of the target's magnetic signature (signal) on the magnetic background noise itself. The noise is used to filter the composed signal (noise+signal) and extract the target signal, thus detecting the threat presence by means of a differential technique (Faggioni et al., 2010; Faggioni et al., 2009b).

The effectiveness of the processing algorithm depends on the deployment of the magnetic field measurement points. Magnetic sensors must ensure, at the same time, 1) correlation among the various noise measurements (reference devices: all the magnetometers record the same background field, which has low spatial frequency and therefore remains approximately constant in a wide area), and 2) de-correlations in the target signal observations (sentinel device: only one sensor records the target signature, which is characterized by high spatial frequency) (Bartels et al., 1939; Cafarella et al., 1992; Cafarella and Meloni, 1995; Chapman, 1918; De Santis et al., 1997; De Santis et al., 2003; Georgieva et al., 2013; Meloni et al., 1994; Meloni et al., 2007).

In conclusion, sensors must be close enough to one another so that they all measure a common background noise, which might be modelled as a constant that does not carry information. This is in accordance with the so-called space stability of the magnetic noise. In other words, in the test area the spatial gradient of the temporal component of the measured magnetic noise nullifies. At the same time, the sensors should lie distant enough from one another so that just one sensor measures the target signal. One should keep in mind that a magnetic anomaly extends over a certain surrounding space, which depends on the amplitude of the signal itself: singularities featuring greater amplitudes occupy a larger volume. Therefore, to detect targets of stronger signatures would be necessary to increase the distance between the sensors. As a matter of fact, the optimal distance, L, between each pair of sensors is determined on the basis of the magnetic characteristics of the expected target sources (in particular the spatial wavelength of the weakest magnetic source: geometric factor) and the physical characteristics of sea water, in particular salinity (environmental factor). Therefore, L is a calibration parameter which is verified experimentally during the system deployment (usually $L < 10$ m). To detect stronger sources one just considers pairs of sensors that lie from each other at distances 2 L, 3 L, and so on, thus simulating the increase in the distance between the sensors.

The system setup involves the deployment along a straight line of N magnetometers on the sea bottom where a diver is expected to float, as shown in Fig. 1. For a given value of L, the number of sensors, N, depends on the size of the area to be protected. The cable carries sensor data to a control unit (workstation and interface placed on a pier near the trials area) for further processing.

The distance, L, between sensors in the array ensures the detection of a bottom-skimming diver at most some meters from the barrier. If a target increases its clearance from the sea floor, it also increases its distance from the sensors and progressively leaves the magnetic detection area (but enters the operating field of sonar systems). The maximum distance at which each target can be detected depends on the type of magnetic source it represents.

Then, the detection algorithm (based on a differential technique) extracts anomalies due to target passages. Fig. 2 illustrates the processing procedure in the case of an elementary cell (only $N = 3$ sensors). To decide if an alarm should be generated on sensor n. 1, the signal acquired by the sensor itself is compared with that of the sensor n. 2; if the difference exceeds a threshold value, an alarm is generated; otherwise the comparison with the sensor n. 3 is performed; also in this case an alarm is generated if the difference exceeds the threshold; if no difference exceeds the threshold value no alarm is generated (the sensor n.

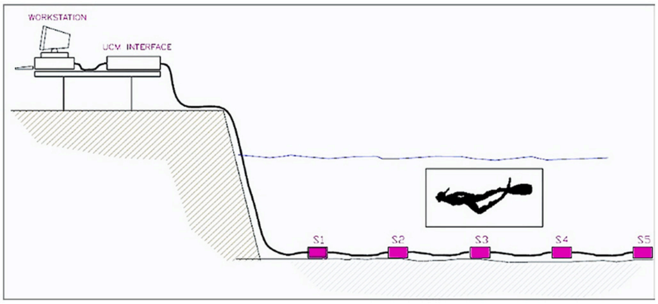

Fig. 1. Scheme of the system deployed at sea.

---

[1] Coastal Anti -Intruders MAgnetometers Network

[2] LAnd / MArine magnetometric detector for self informed systems

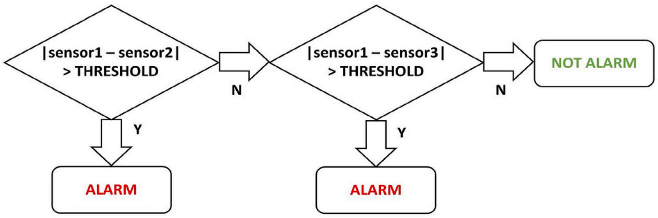

Fig. 2. Flow chart of the detection algorithm for the elementary cell.

1 does not differ significantly from the background noise level).

The hypothesis of space stability of the magnetic noise might no longer hold in the case of very long barriers; in this case, the solution is to divide the array into several, independent sub-systems capable of generating alarms. To dimension the length of each subsystem, one should assess, during the setup phase, within what distance all sensors measure the same noise; in a port environment, that distance usually lies in the order of hundreds / thousands of meters.

A generalized, multi-sensor configuration allows to sort out the anomalies (singularities) generated by the transits of different targets from the background field (noise): the data acquired by each sensor are compared with those recorded by all the other magnetometers (Faggioni, 2018; Faggioni, 2019; Kanasewich, 1981; Telford et al., 1990). In particular, the comparisons between signals from adjacent sensors will highlight the presence of small magnetic anomalies (e.g. generated by divers). On the other hand, the comparisons between farther sensors will help identify larger magnetic anomalies (observed simultaneously by multiple sensors). This occurs, for example, when a pair of divers approach together or are aided by an underwater vehicle. When a diver passes halfway between two sensors, the magnetometers lying at a larger distance than L are not affected by the presence of targets and are used as reference sensors. Then, anomalies are compared with threshold levels to generate alarms.

A software application (developed in C++ language) runs on the control unit; it processes the data acquired by all the magnetometers in real-time, and turns on a visual and an acoustical (beep) alert when a magnetic anomaly is identified; the sensors not involved in the event remain green and silent; Fig. 3 shows the user interface.

2.2. The sensor hardware

Fig. 4 presents the sensor placed on a laboratory floor. The magnetometer is housed in a waterproof box, IP68, tested at a depth of 10 m for 8 h. The box is secured to a PVC block to ensure a stable installation on the sea bottom and adequate resistance to sea currents.

The magnetometer is based on the A1015 dual-axis fluxgate produced by Autonnic (see https://www.autonnic.com/, accessed 18 January 2022); it measures the components of the magnetic field along two directions X and Z, as shown in Fig. 5. The X axis is arranged according to the direction along which the array is deployed, whereas the

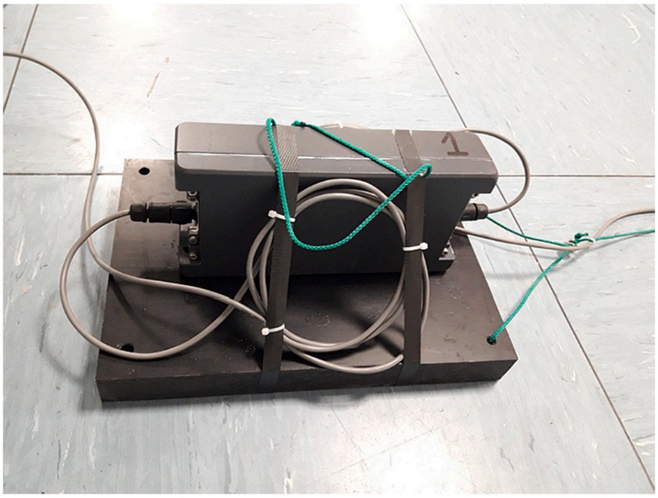

Fig. 4. The magnetometer on the laboratory floor.

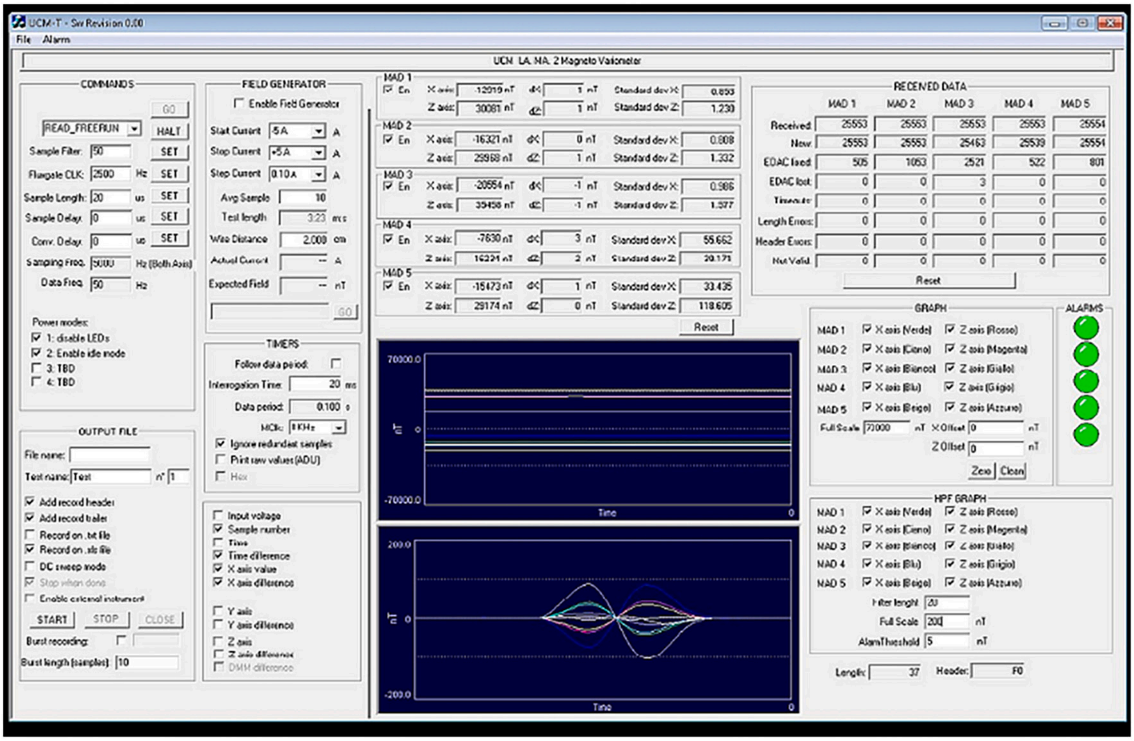

UCM-T - Sw Revision 0.00

UCM LA. MA. 2 Magneto Valiometer

COMMANDS

READ_FREERUN

Sample Filter: 50

Fluxgate CLK: 2500 Hz

Sample Length: 20 us

Sample Delay: 0 us

Conv. Delay: 0 us

Sampling Freq. 5000 Hz (Both Axis)

Data Freq. 50 Hz

Power modes:
☑ 1: disable LEDs
☑ 2: Enable idle mode
☐ 3: TBD
☐ 4: TBD

FIELD GENERATOR

☐ Enable Field Generator

Start Current -5A A

Stop Current +5A A

Step Current 0.10A A

Avg Sample 10

Test length 3:23 m:s

Wire Distance 2.000 cm

Actual Current -- A

Expected Field -- nT

TIMERS

Follow data period: ☐

Interogation Time: 20 ms

Data period: 0.100 s

MClk: 1KHz

☑ Ignore redundant samples
☐ Print raw values (ADU)
☐ Hex

OUTPUT FILE

File name:

Test name: Test n° 1

☑ Add record header
☑ Add record trailer
☐ Record on .txt file
☑ Record on .xls file
☐ DC sweep mode
☑ Stop when done
☐ Enable external instrument

Burst recording: ☐

Burst length (samples): 10

☐ Input voltage
☑ Sample number
☐ Time
☑ Time difference
☑ X axis value
☑ X axis difference
☐ Y axis
☐ Y axis difference
☐ Z axis
☐ Z axis difference
☐ DMM difference

MAD 1 ☑ En	X axis: -12019 nT	dX: 1 nT	Standard dev X: 0.853
	Z axis: 30081 nT	dZ: 1 nT	Standard dev Z: 1.230
MAD 2 ☑ En	X axis: -16321 nT	dX: 0 nT	Standard dev X: 0.808
	Z axis: 29968 nT	dZ: 1 nT	Standard dev Z: 1.332
MAD 3 ☑ En	X axis: -20554 nT	dX: -1 nT	Standard dev X: 0.986
	Z axis: 35458 nT	dZ: -1 nT	Standard dev Z: 1.577
MAD 4 ☑ En	X axis: -7630 nT	dX: 3 nT	Standard dev X: 55.662
	Z axis: 16224 nT	dZ: 2 nT	Standard dev Z: 20.171
MAD 5 ☑ En	X axis: -15473 nT	dX: 1 nT	Standard dev X: 33.435
	Z axis: 29174 nT	dZ: 0 nT	Standard dev Z: 118.605

RECEIVED DATA

	MAD 1	MAD 2	MAD 3	MAD 4	MAD 5
Received	25553	25553	25553	25553	25554
New	25553	25553	25463	25539	25554
EDAC fixed	505	1063	2521	522	801
EDAC lost	0	0	3	0	0
Timeouts	0	0	0	0	0
Length Errors	0	0	0	0	0
Header Errors	0	0	0	0	0
Not Valid	0	0	0	0	0

GRAPH

MAD 1 ☑ X axis (Verde) ☑ Z axis (Rosso)
MAD 2 ☑ X axis (Ciano) ☑ Z axis (Magenta)
MAD 3 ☑ X axis (Bianco) ☑ Z axis (Giallo)
MAD 4 ☑ X axis (Blu) ☑ Z axis (Grigio)
MAD 5 ☑ X axis (Beige) ☑ Z axis (Azzurro)

Full Scale 70000 nT X Offset 0 nT

Z Offset 0 nT

ALARMS

HPF GRAPH

MAD 1 ☑ X axis (Verde) ☑ Z axis (Rosso)
MAD 2 ☑ X axis (Ciano) ☑ Z axis (Magenta)
MAD 3 ☑ X axis (Bianco) ☑ Z axis (Giallo)
MAD 4 ☑ X axis (Blu) ☑ Z axis (Grigio)
MAD 5 ☑ X axis (Beige) ☑ Z axis (Azzurro)

Filter lenght 20

Full Scale 200 nT

AlarmThreshold 5 nT

Length: 37 Header: F0

Fig. 3. The user interface.

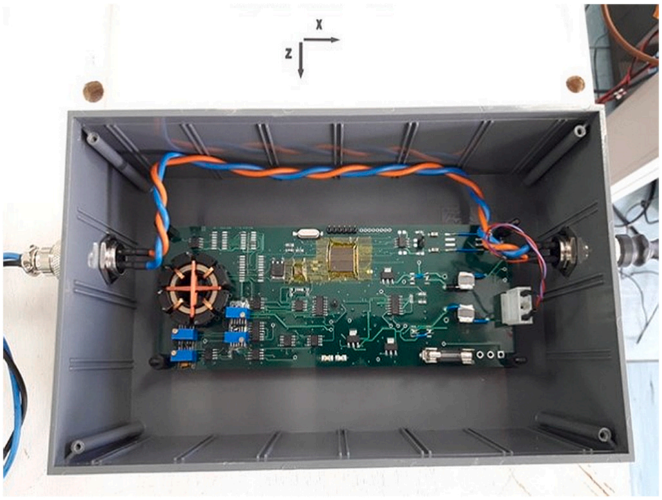

Fig. 5. The inside of the magnetometer and the directions of its axis.

Z axis is set perpendicular to the seabed and directed to the centre of the Earth. The sensor is sensitive to changes in the field (the method considers the variations of the magnetic field and not its total value). Due to the geometry of the array, the characteristics of the Earth's magnetic field, and the trajectories described by targets, the Z component is usually most adequate to read the anomalies induced by a target's transit. This justifies the choice of the low cost, dual-axis commercial sensor, and explains why the Z component is used in the presented graphs.

One serial cable traverses all sensors and transmits the carries data to the shore unit; it also provides power supply to each sensor. Overall, the system dissipates about 100 W (sensors at sea + control unit on land) and can be powered by a 24 V battery; since the sensors are passive, the magnetometer network can be considered as having almost zero impact on the surrounding environment. The sampling frequency of 10 Hz, the sensitivity of 0.1 nT and the data resolution of 1 nT meet the present requirements, since the goal is target detection rather than the measurement of the total magnetic field.

3. Results

In February 2019, at the end of the LAMA2.0 Project, operational tests on the magnetometer system (including $N = 5$ sensors) were carried out in the Bay of Santa Teresa, Gulf of La Spezia (Italy; see Fig. 6), characterized by medium-high environmental noise (the artificial component due to activity of port and industrial plants overlaps the natural noise due to Earth's magnetic field).

Fig. 7 shows the diver preparation phase on the pier, while Fig. 8 is a picture taken at the seabed (at nearly 7.5 m depth).

Fig. 9 shows the signals generated (Z component of magnetic field) by a diver equipped with a steel tank (well detectable by magnetic sensors) swimming back and forth at approximately 1.5 m above the system.

Then, data were filtered, since one is interested in the variations of the field rather than in its total value: the median value of a sliding window of appropriate size was subtracted from each sample: the filtering eliminated the background level (which did not carry useful information) and some environmental slow variations (see Fig. 10).

The diver's transit was well detected by each magnetometer (first from sensor 1 to sensor 5, then from 5 to 1): the scuba was swimming at a distance approximately between 1 and 2.5 m from the magnetometers (the diver was moving at variable depth and not exactly along the linear array), the system could detect the presence of a scuba equipped with a steel tank up to a distance of about 5 m. The difference in pulse amplitude depended on the different distances of the diver from the array elements, whereas the duration of each pulse varied with the diver's speed. The interval between consecutive pulses was caused by the fact that the diver, despite having to pass above the sensors to test the system, temporarily drifted away up to several meters from the array due to poor visibility on the sea bottom (simulating operational conditions, where the diver does not know the position of the sensors). Finally, the different shape of the pulse (positive, negative, dipole) depended on how the diver approached the magnetometer axes.

The system could detect the presence of much weaker magnetic sources, as shown in Fig. 11, which corresponds to tests in which a diver was equipped with an aluminium tank (a portion of the scuba's equipment still remained magnetic-sensitive, e.g. the air regulator); in this test, the scuba was passing twice over the barrier, at approximately 1.5

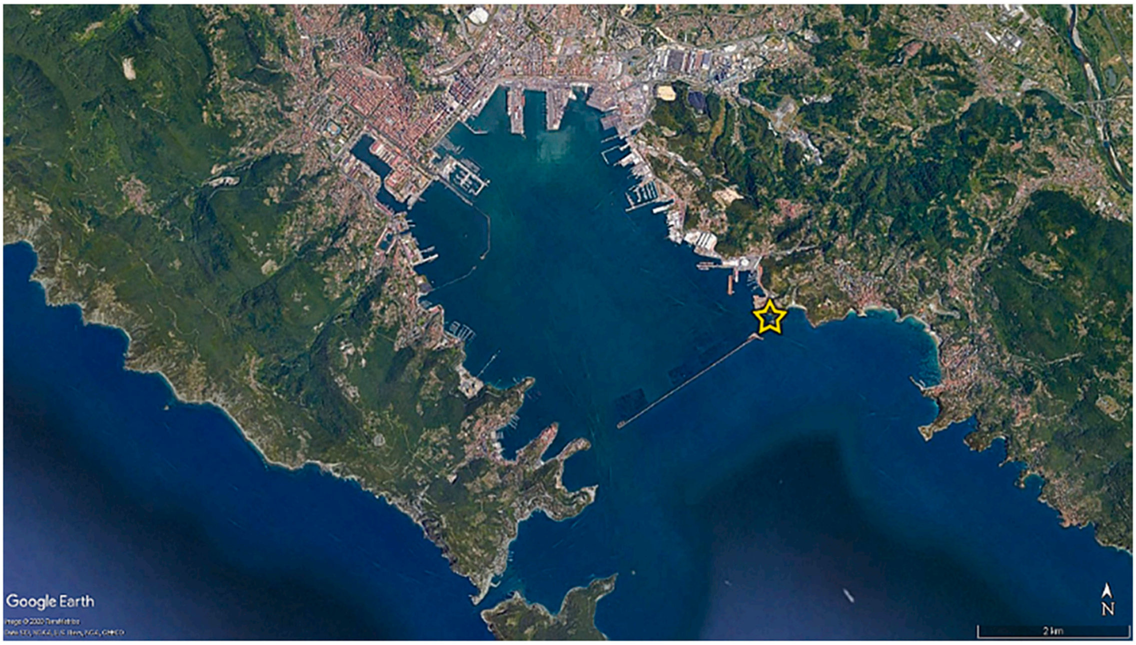

Fig. 6. Harbour of La Spezia (Northern Italy); the yellow star indicates the test site (picture from Google Earth). (For interpretation of the references to colour in this figure legend, the reader is referred to the web version of this article.)

Fig. 7. The diver on the pier.

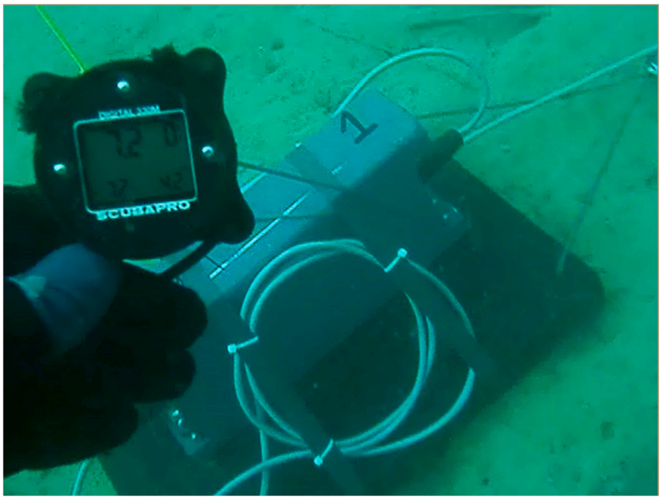

Fig. 8. At the sea bottom, above the sensor n. 1.

m above the sensor n. 2.

As shown in Fig. 11, the target's weak signal remained hidden in the high background noise, but by applying the filtering, the diver passages became apparent (see Fig. 12).

In this case, the system faced similar pulses (in amplitude and duration) during the first half of the acquisition: the pulses highlighted by green ovals were classified by the analysis algorithm as background noise because all five magnetometers had been “disturbed” in the same way (no alarm). On the contrary, the real-time processing procedure reported the red pulse as an alarm as well as the great red dipole at the end of the recording, because they had been measured by one magnetometer and therefore were considered anomalies with respect to the background noise: that pointed out the presence of the diver (see in Fig. 13 anomalies identified by the detection algorithm for the experiment in Fig. 12).

The whole process is ruled by suitable threshold levels (threshold values between environmental noise level and signal peaks are satisfactory). In the example, two alarms were triggered when two peaks exceed the threshold level.

In this video, we have combined a movie shot by the diver (equipped with a steel tank) with the anomalies generated by himself (the magnetic source is essentially represented by the scuba tank, while the camera is held by the diver in his hand); the diver starts about 3 m above sensor 5 (coming from the rise above sensor 4), then runs along the barrier from sensor 5 to 1.

Fig. 14 shows the alarms generated while a diver was crossing the barrier swimming first above the sensor n. 1 and then halfway between the sensors n. 2 and n. 3. Red hexagons correspond to sensors alarmed; red hexagons joined by the red bar identify an anomaly involving two sensors at the same time.

Fig. 17 shows the signals (after the filtering) acquired during the passage of the diver (equipped with an aluminium tank) on board the vehicle shown in Figs. 15 and 16 (also made of aluminium, and equipped with an electric motor) some meters above the array: as can be seen, during two passages the target affects multiple sensors at a time.

The system correctly detected the anomalies induced by the target; in that case, the system used as reference sensors a subset of magnetometers lying at higher distances than L, which were not affected by the transit of the manned vehicle (see Fig. 18).

In the case of multisensorial harbour protection (appropriately integrated systems so that the shadow areas of each one are filled by others), each alarm generated was forwarded to a command and control central station, which collected the alarms received by all sub-systems (magnetic, acoustic, optical, infrared, electrical, radar, etc.).

4. Discussion and conclusions

The paper described the development of an underwater magnetometer self-informed network for harbour protection purposes. The experimental tests, in undersea environments with high magnetic noise, confirmed extremely positive operational results in the detection of transiting intruders; the experiments covered divers equipped both with steel and aluminium tanks, or on board underwater vehicles. As opposed to other systems (not based on this differential technique), the real-time analysis algorithm could discriminate the target signals from the environmental background noise, even if characterized by similar amplitudes.

The percentage of false alarms (value of false positive rate) depends on the distance of the target from the system; in general, during the test a rate of <10% was found (the maximum value refers to a diver swimming near the edge of the working area).

As compared to the previous versions of the system, self-designed proprietary sensor allowed to reduce costs, and therefore develop a larger number of magnetometers to protect wider areas. The interconnections through a single cable makes the deployment at sea easier and faster and provide a baud rate of about 1 Mbit / *sec*. Its elements (sensors, resin treatment) were tested at a depth of 10 m. Finally, the system has a very low impact on the surrounding environment and dissipates only about 100 W.

In the context of antiterrorism systems for harbour protection, the magnetic network is a useful complement to the acoustic component in the peripheral ‘shadow’ areas close to the seabed or docks. For the global surveillance of a wide port area, magnetic and acoustic systems can integrate with other systems, such as radar systems or infrared cameras to monitor the sea surface.

In an operational scenario, a picture showing the area under

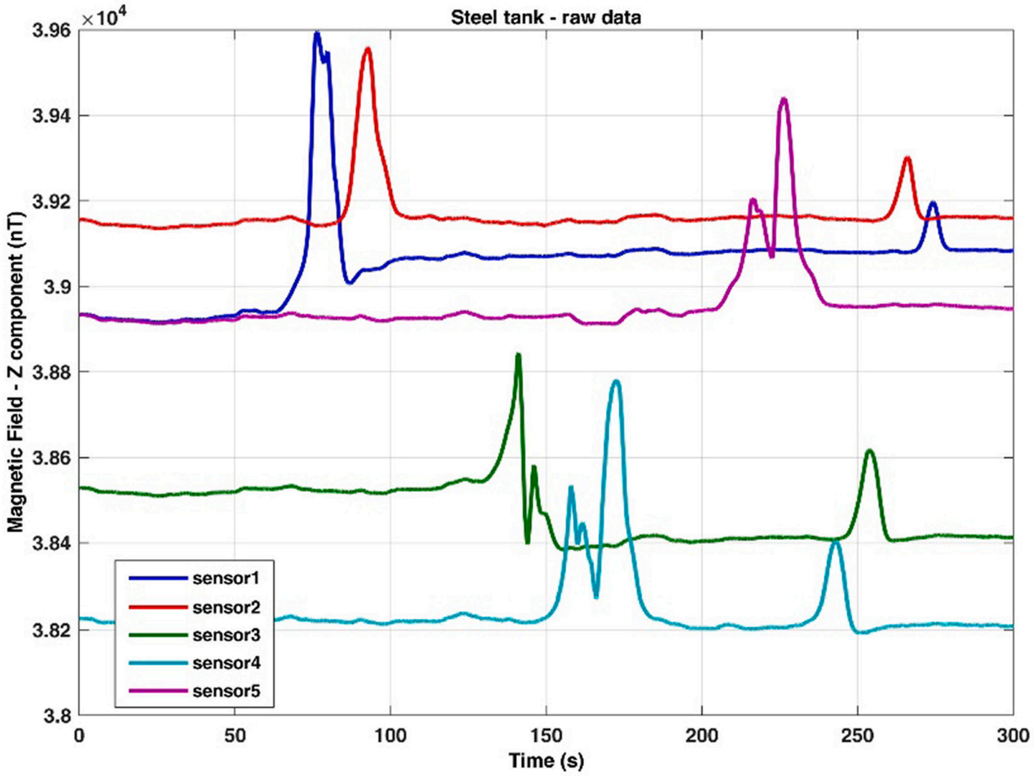

Fig. 9. Magnetic signals generated by a diver equipped with a steel tank.

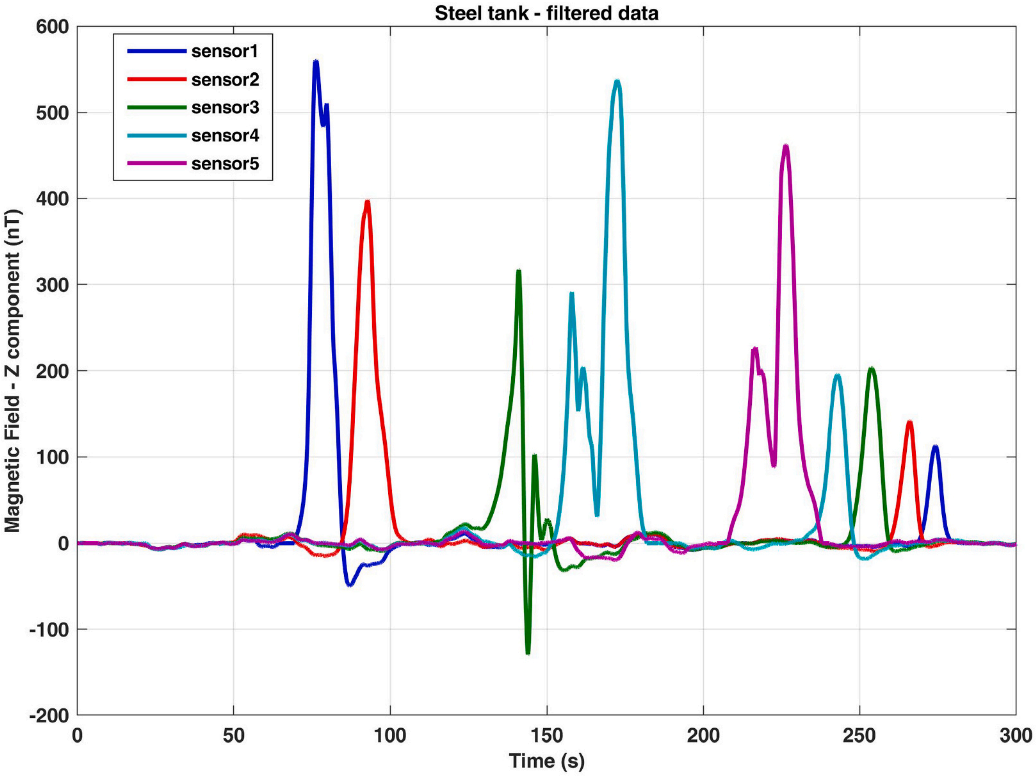

Fig. 10. Filtered magnetic signals generated by a diver equipped with a steel tank.

surveillance could be placed in a command and control centre managed by local authorities, to provide useful support to security-responsible decision-makers.

The locations of the magnetometers on the sea bottom are well-known, hence real-time alarms received from the software application can be represented by means of red points on the map of the port, as

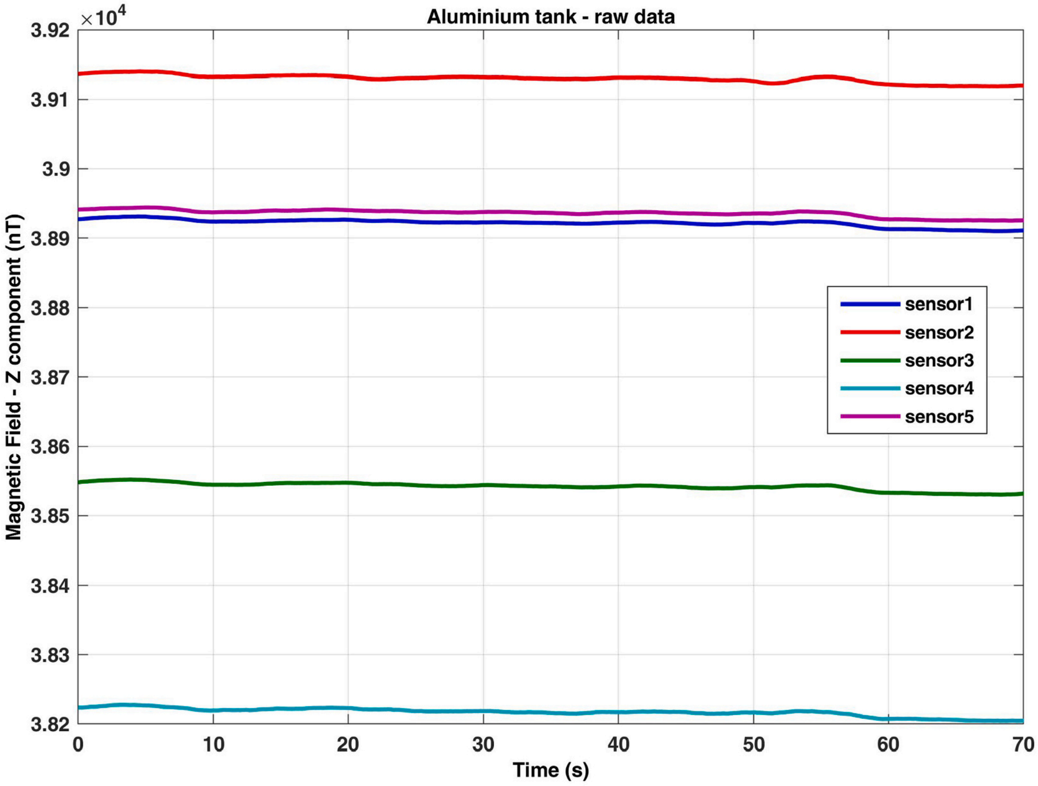

Fig. 11. Magnetic signals generated by a diver equipped with an aluminium tank.

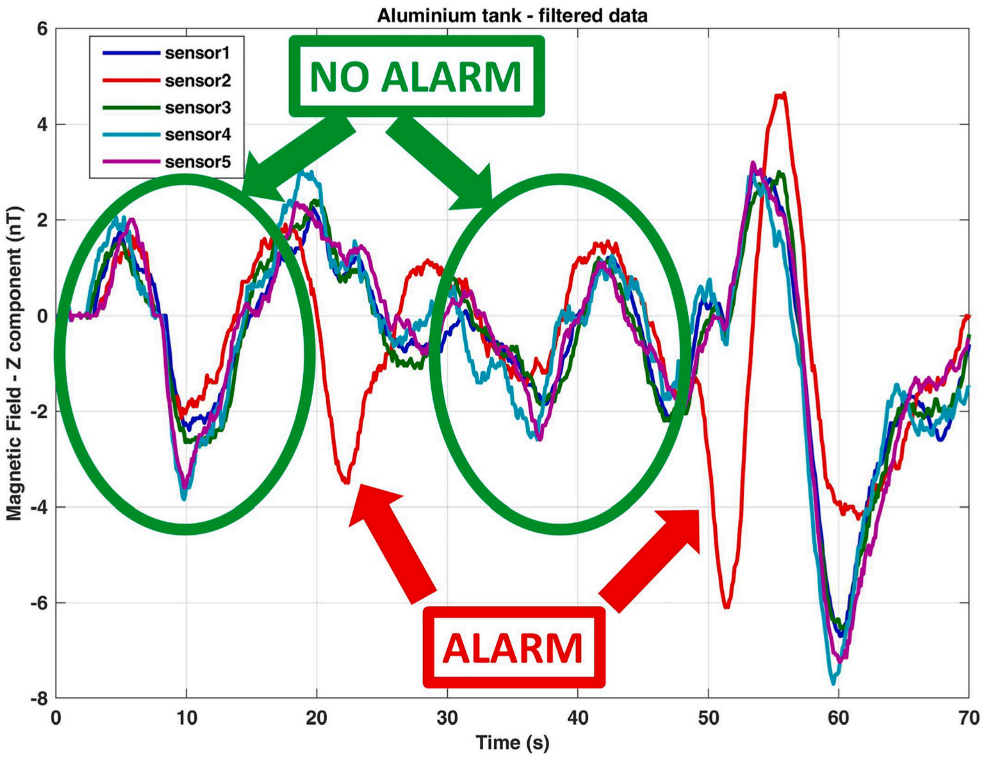

Fig. 12. Filtered magnetic signals generated by a diver equipped with an aluminium tank.

shown in Fig. 19. The white line shows a test run back and forth performed by the diver above the central sensor (n. 3), the red point represents the sensor sending an alarm, the green ones indicate magnetometers not alarmed. The sensor started to send the alarm when the diver was about 3 m from the barrier and it stopped when he was nearly 3 m beyond (red segments of the tracks).

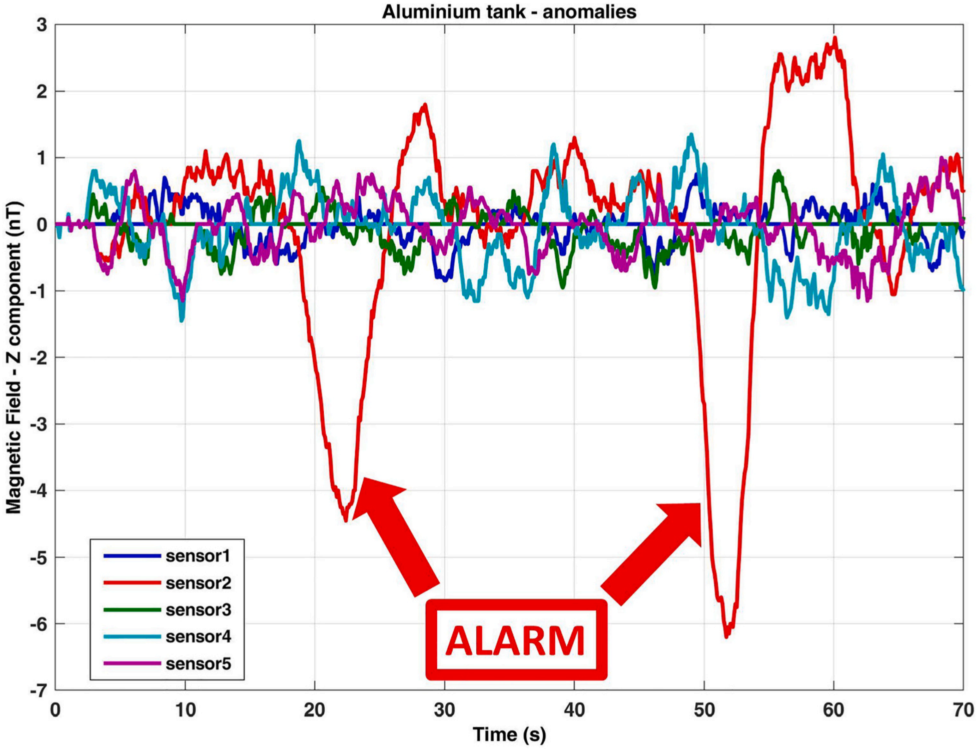

Fig. 13. Magnetic anomalies generated by a diver equipped with an aluminium tank.

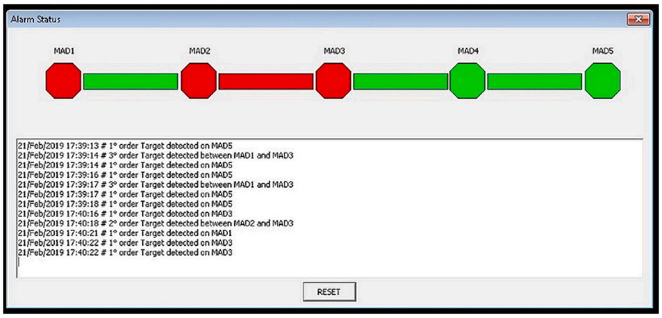

```
21/Feb/2019 17:39:13 # 1° order Target detected on MAD5
21/Feb/2019 17:39:14 # 3° order Target detected between MAD1 and MAD3
21/Feb/2019 17:39:14 # 1° order Target detected on MAD5
21/Feb/2019 17:39:16 # 1° order Target detected on MAD5
21/Feb/2019 17:39:17 # 3° order Target detected between MAD1 and MAD3
21/Feb/2019 17:39:17 # 1° order Target detected on MAD5
21/Feb/2019 17:39:18 # 1° order Target detected on MAD5
21/Feb/2019 17:40:16 # 1° order Target detected on MAD3
21/Feb/2019 17:40:18 # 2° order Target detected between MAD2 and MAD3
21/Feb/2019 17:40:21 # 1° order Target detected on MAD1
21/Feb/2019 17:40:22 # 1° order Target detected on MAD3
21/Feb/2019 17:40:22 # 1° order Target detected on MAD3
```

Fig. 14. The alarm window; alarms generated by a diver.

Fig. 15. Manned underwater vehicle.

The tests gave very satisfactory results, and at the end of the LAMA2.0 Project, the system prototype was delivered to the Italian Ministry of Defence. In the wake of the success of this first prototype, the consortium intends to extend the one-dimensional concept of barrier network to a 2-D matrix layout of sensors, capable of both detecting and tracking possible threats at the same time. Moreover, since the sensors are all interconnected and already exchange the signals they acquire, we plan to partially distribute the processing load, moving it from the control station to each sensor, which would no longer be a simple magnetometer but becomes an actual and faster detector.

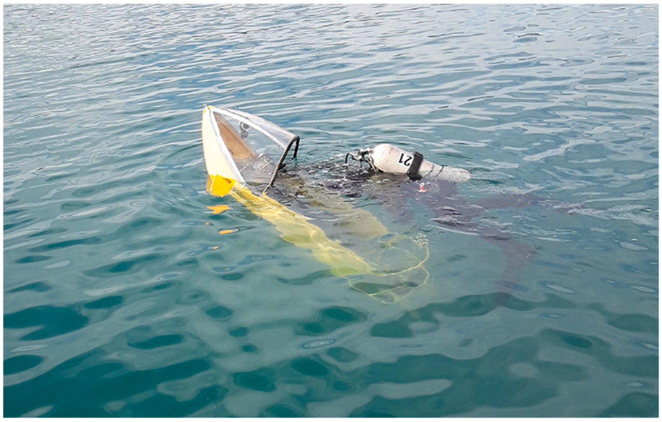

Fig. 16. The diver as he gets on the vehicle.

Supplementary data to this article can be found online at https://doi.org/10.1016/j.jappgeo.2022.104743.

CRediT authorship contribution statement

Maurizio Soldani: Conceptualization, Data curation, Formal analysis, Funding acquisition, Investigation, Methodology, Software, Validation, Writing – original draft, Writing – review & editing. **Osvaldo Faggioni:** Conceptualization, Formal analysis, Funding acquisition, Investigation, Methodology, Supervision, Validation, Visualization, Writing – review & editing. **Rodolfo Zunino:** Conceptualization, Formal analysis, Funding acquisition, Resources, Investigation, Methodology, Software, Writing – review & editing. **Alessandro Carbone:**

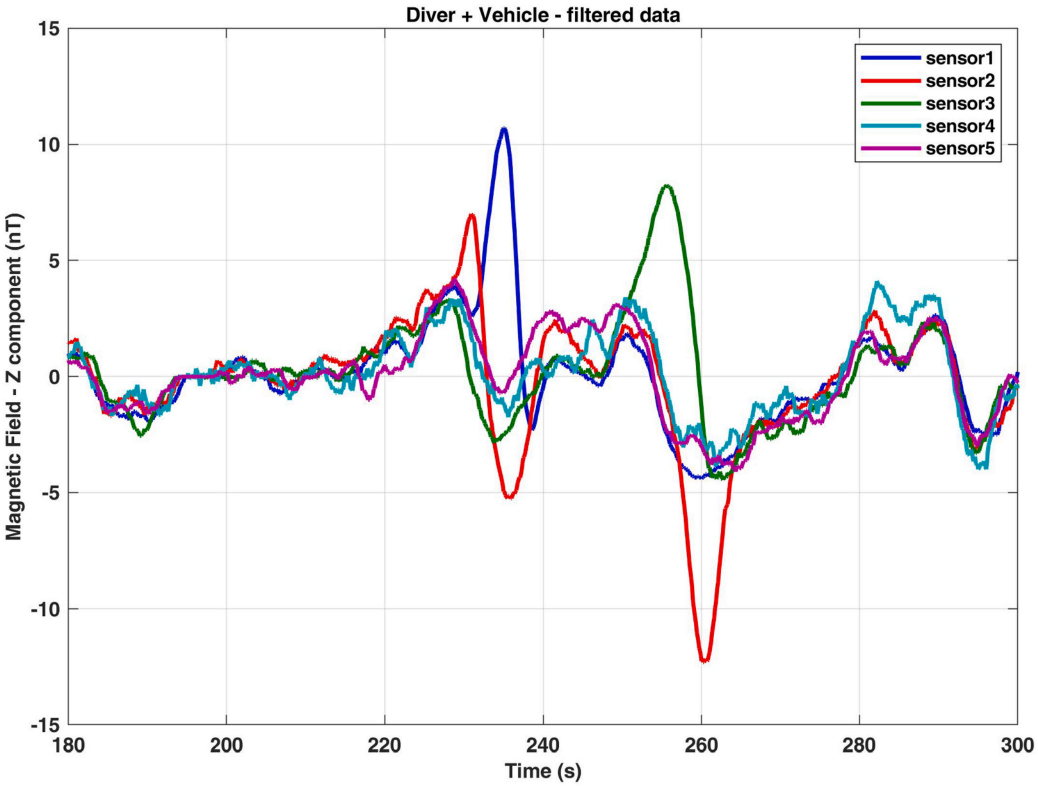

Fig. 17. Filtered magnetic signals generated by a diver on board the underwater vehicle.

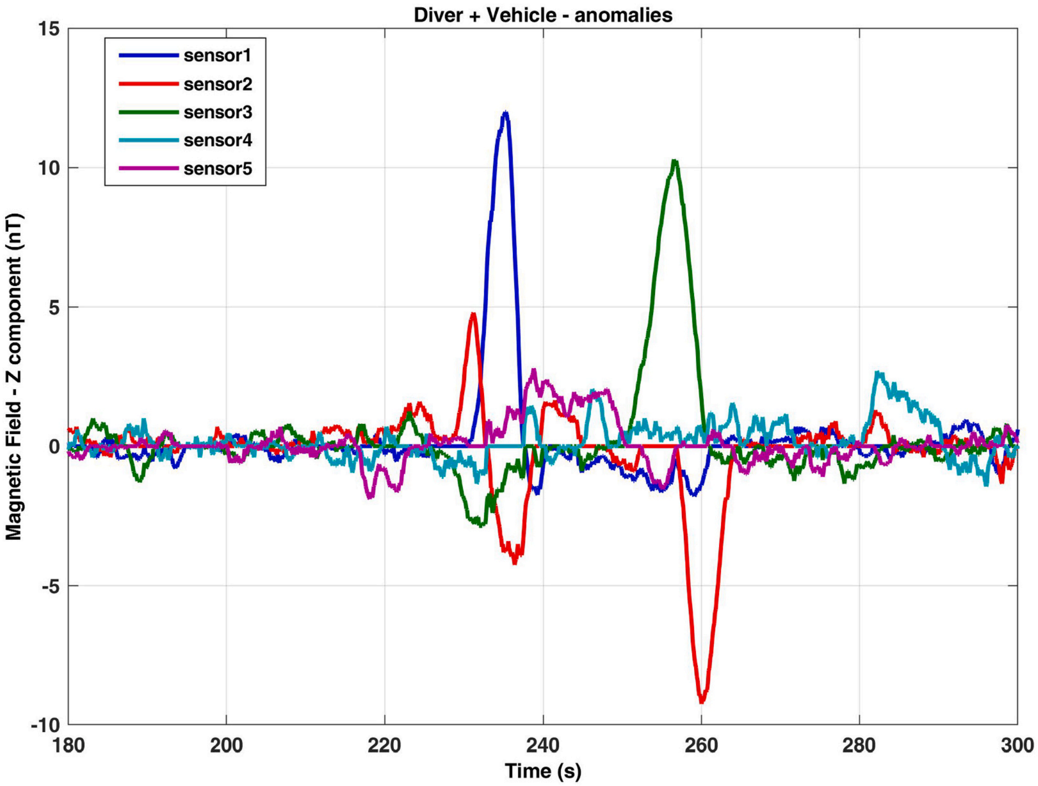

Fig. 18. Magnetic anomalies generated by a diver on board the underwater vehicle.

Conceptualization, Data curation, Funding acquisition, Project administration, Resources, Software, Visualization, Writing – review & editing. **Marco Gemma:** Conceptualization, Data curation, Formal analysis, Funding acquisition, Project administration, Resources, Software, Visualization, Writing – original draft, Writing – review & editing.

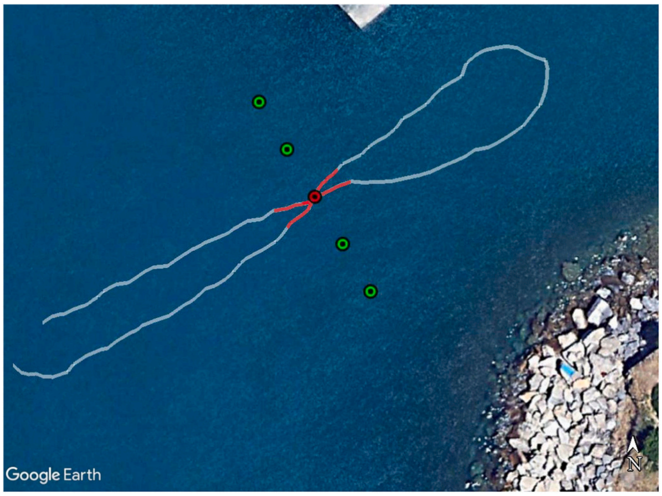

Fig. 19. The magnetic system and the track of the diver; red: sensor alarmed, green: sensors not alarmed (picture modified from Google Earth). (For interpretation of the references to colour in this figure legend, the reader is referred to the web version of this article.)

Declaration of Competing Interest

The authors declare that they have no known competing financial interests or personal relationships that could have appeared to influence the work reported in this paper.

Acknowledgments

The authors wish to thank the “Scuola di Mare Santa Teresa” (La Spezia, Italy) for hosting sea trials, and Telesub Lanterna (La Spezia, Italy) for their support in carrying out the sea trials themselves. They also wish to thank the WASS Company (now Leonardo, Livorno) for its original contribution in the development of the CAIMAN system.

The authors gratefully acknowledge grants by the Italian Ministry of Defence, which made these studies possible.

References

Bartels, J., Heck, N.H., Johnston, H.F., 1939. The three-hour-range index measuring geomagnetic activity. Terr. Magn. Atmos. Electr. 44 (4), 411–454. https://doi.org/10.1029/TE044i004p00411.

Cafarella, L., Meloni, A., 1995. Evidence for a geomagnetic jerk in 1990 across Europe. Ann. Geofis. 38 (3–4), 451–455. https://doi.org/10.4401/ag-4106.

Cafarella, L., De Santis, A., Meloni, A., 1992. Secular variation in Italy from historical geomagnetic field measurements. Phys. Earth Planet. Inter. 73 (3–4), 206–221. https://doi.org/10.1016/0031-9201(92)90091-9.

Chapman, S., 1918. The diurnal changes of the Earth's magnetism. Observatory 41, 52–60.

De Santis, A., Chiappini, M., Dominici, G., Meloni, A., 1997. Regional geomagnetic field modelling: the contribution of the Istituto Nazionale di Geofisica. Ann. Geofis. 40 (5), 1161–1169. https://doi.org/10.4401/ag-3854.

De Santis, A., Gaya-Piqué, L., Dominici, G., Meloni, A., Torta, J.M., Tozzi, R., 2003. ITalian Geomagnetic Reference Field (ITGRF): update for 2000 and secular variation model up to 2005 by autoregressive forecasting. Ann. Geophys. 46 (3), 491–500. https://doi.org/10.4401/ag-3422.

De Vuyst, A., De Meyer, F., 1973. Spectral Analysis of Geomagnetic Data from One Station (Dourbes 1960-1970). *Institut Royal Météorologique de Belgique Publications*, Bruxelles. A, 80.

Dobkowski, J.T., Cichocki, R., Szarkowski, F., 2007. Deployable magnetic barrier for detection of underwater terrorist threat. In: CD-ROM Proceedings of UDT Europe 2007 Conference. June 5-7, Naples, Italy.

Dobkowski, J.T., Chodkiewicz, H., Szarkowski, F., 2008. Detection of drifting mines and other types of asymmetric threats with the application of magnetic barriers. In: CD-ROM Proceedings of UDT Europe 2008 Conference. June 11-13, Glasgow, UK.

Faggioni, O., 2018. The Fourier notation of the geomagnetic signals informative parameters. J. Signal Inf. Process. 9, 153–166. https://doi.org/10.4236/jsip.2018.93009.

Faggioni, O., 2019. The information protection in automatic reconstruction of not continuous geophysical data series. J. Data Anal. Inf. Process. 7, 208–227. https://doi.org/10.4236/jdaip.2019.74013.

Faggioni, O., Gabellone, A., Hollett, R., Kessel, R.T., Soldani, M., 2008. Anti-intruder port protection “MAC (Magnetic ACoustic) System”: advances in the magnetic component performance. In: *CD-ROM Proceedings of 1stWSS Conference*. August 25-28, Copenhagen, Denmark.

Faggioni, O., Soldani, M., Gabellone, A., Maggiani, P., Leoncini, D., 2009a. Development of anti intruders underwater systems: time domain evaluation of the self-informed magnetic networks performance. In: Corchado, E., Zunino, R., Gastaldo, P., Herrero, Á. (Eds.), Proceedings of the International Workshop on Computational Intelligence in Security for Information Systems CISIS 2008. Springer-Verlag, Berlin Heidelberg, Germany, pp. 100–107. https://doi.org/10.1007/978-3-540-88181-0_13. *Advances in Soft Computing*, 53.

Faggioni, O., Soldani, M., Leoncini, D., Gabellone, A., Maggiani, P.V., 2009b. Time domain performances analysis of underwater magnetic SIMAN Systems for port protection. J. Inf. Assur. Secur. 4 (6), 538–545. Special Issue on Information Assurance and Data Security.

Faggioni, O., Soldani, M., Zunino, R., Leoncini, D., Di Gennaro, E., Gabellone, A., Maggiani, P.V., Falcucci, V., Michelizza, E., 2009c. Building the synthetic “MAC System”: an analytical integration of magnetic and acoustic subsystems for port protection scenarios. In: CD-ROM Proceedings of UDT Europe 2009 Conference. June 9-11, Cannes, France.

Faggioni, O., Soldani, M., Gabellone, A., Hollett, R.D., Kessel, R.T., 2010. Undersea harbour defence: a new choice in magnetic networks. J. Appl. Geophys. 72 (1), 46–56. https://doi.org/10.1016/j.jappgeo.2010.07.001.

Faggioni, O., Soldani, M., Cozzani, G., Zunino, R., 2018. Informative signal analysis: metrology of the underwater geomagnetic singularities in low-density ionic solution (sea water). J. Signal Inf. Process. 9 (1), 1–23. https://doi.org/10.4236/jsip.2018.91001.

Gabellone, A., Faggioni, O., Soldani, M., Guerrini, P., 2007. CAIMAN experiment. In: CD-ROM Proceedings of UDT Europe 2007 Conference. June 5-7, Naples, Italy.

Gavazzi, B., Le Maire, P., de Lépinay, J.M., Calou, P., Munschy, M., 2019. Fluxgate three-component magnetometers for cost-effective ground, UAV and airborne magnetic surveys for industrial and academic geoscience applications and comparison with current industrial standards through case studies. Geomech. Energy Environ. 20, 100117. https://doi.org/10.1016/j.gete.2019.03.002.

Georgieva, K., Kirov, B., Nagovitsyn, Y.A., 2013. Long-term variations of solar magnetic fields derived from geomagnetic data. Geomagn. Aeron. 53 (7), 852–856. https://doi.org/10.1134/S0016793213070062.

Hirvi, K., Huoman, K., Poikonen, A., 2007. Magnetic harbour entrance protection and surveillance system. CD-ROM Proceedings of UDT Europe 2007 Conference. June 5-7, Naples, Italy.

Kanasewich, E.R., 1981. Time Sequence Analysis in Geophysics, 3rd edn. University of Alberta, Canada.

Lipovský, P., Draganová, K., Šmelko, M., Volčko, T., 2015. Vector magnetometer used as magnetometric security subsystem. In: Proceedings of International Conference on Military Technologies (ICMT) 2015. May 19-21, Brno, Czech Republic.

Liu, D., Xu, X., Huang, C., Zhu, W., Liu, X., Yu, G., Fang, G., 2015. Adaptive cancellation of geomagnetic background noise for magnetic anomaly detection using coherence. Meas. Sci. Technol. 26 (1), 015008. https://doi.org/10.1088/0957-0233/26/1/015008.

Meloni, A., Battelli, O., De Santis, A., Dominici, G., 1994. The 1990.0 magnetic repeat station survey and normal reference fields for Italy. Ann. Geofis. 37 (5), 949–967. https://doi.org/10.4401/ag-4185.

Meloni, A., Cafarella, L., De Michelis, P., De Santis, A., Di Mauro, D., Dominici, G., Lepidi, S., Palangio, P., Tozzi, R., Zirizzotti, A., 2007. Systematic magnetic observations in Italy. Publ. Inst. Geophys. Pol. Acad. Sci. C-99 (398), 8.

Nasta, S., Faggioni, O., Soldani, M., 2015. Underwater magnetometric detection of quasi-punctiform kinematic sources: from the metrology of the field to the metrology of the singularity. In: CD-ROM Proceedings of MTS/IEEE OCEANS’15 Conference. https://doi.org/10.1109/OCEANS-Genova.2015.7271389. May 18–21, Genoa, Italy.

NOAA, et al., 2010. NOAA Diving Manual: Diving for Science and Technology, 4th Edn Revised. Best Publishing Company, North Palm Beach, Florida.

Serkerov, S.A., Tsvetkov, Y.P., Kharitonov, A.L., 1996. Application of the method of mutual correlation functions to interpret data of gradient magnetic surveys. Geomagn. Aeron. 35 (6), 867–870.

Szarka, L., 1988. Geophysical aspects of man-made electromagnetic noise in the earth - a review. Surv. Geophys. 9, 287–318. https://doi.org/10.1007/BF01901627.

Telford, W.M., Geldart, P., Sheriff, R.E., 1990. *Applied Geophysics*, 2nd edn. Cambridge University Press, UK. https://doi.org/10.1017/CBO9781139167932.

Tian, Z.X., 2011. Underwater magnetic surveillance system for port protection. In: Proceedings of 2011 IEEE 2nd International Conference on Computing, Control and Industrial Engineering (CCIE). https://doi.org/10.1109/CCIENG.2011.6008013. August 20-21, Wuhan, China.

Wahlström, N., Gustafsson, F., 2014. Magnetometer modeling and validation for tracking metallic targets. IEEE Trans. Signal Process. 62 (3), 545–556. https://doi.org/10.1109/TSP.2013.2274639.

Zhao, Y., Zhang, J., Li, J., Liu, S., Miao, P., Shi, Y., Zhao, E., 2021. A brief review of magnetic anomaly detection. Meas. Sci. Technol. 32 (4) https://doi.org/10.1088/1361-6501/abd055, 042002.